Molecular view of polymer flow into a strongly attractive slit

Arlette R.C. Baljon, Jae Youn Lee, and Roger F. Loring

Citation: The Journal of Chemical Physics **111**, 9068 (1999); doi: 10.1063/1.480248
View online: http://dx.doi.org/10.1063/1.480248
View Table of Contents: http://scitation.aip.org/content/aip/journal/jcp/111/19?ver=pdfcov
Published by the AIP Publishing

Molecular view of polymer flow into a strongly attractive slit

Arlette R.C. Baljon, Jae Youn Lee, and Roger F. Loring
Department of Chemistry and Chemical Biology, Baker Laboratory, Cornell University, Ithaca, New York 14853

(Received 30 July 1999; accepted 23 August 1999)

We present molecular dynamics simulations of the flow of macromolecules from a bulk melt into a slit of nanometer dimension with strongly attracting walls. Such flow is central to the formation of polymer-layered silicate nanocomposites by direct melt intercalation. In this process, polymer molecules flow from a melt into the galleries between the sheets that compose a mica-type layered silicate. We present a systematic study of the effects of polymer molecular weight and polymer-surface interactions on the flow dynamics. © *1999 American Institute of Physics.* [S0021-9606(99)50743-5]

I. INTRODUCTION

Polymer-layered-silicates are nanocomposite materials composed of silicate sheets of approximately 1 nanometer in thickness, separated by polymer-containing galleries, whose thickness is also on the nanometer scale.[1–16] These materials may be formed by annealing layered mica-type silicate minerals with polymer melts. An essential feature of this intercalation process is the motion of macromolecules from a bulk melt into the confining space between silicate sheets. The x-ray diffraction studies of intercalation kinetics by Giannelis *et al.* have shown that the time dependence of the total amount of intercalated polymer can be described by a model in which material diffuses into a slit of fixed volume.[4,5] The effective diffusion coefficient extracted from this analysis, D_{eff}, is typically at least an order of magnitude larger than the self-diffusion coefficient of the same species in a bulk melt. Increasing the affinity of the silicate surface for the polymer, for example, by brominating polystyrene, decreases D_{eff}.[5] For the intercalation of polystyrene into layered silicates whose surfaces are chemically modified by the grafting of short-chain hydrocarbons, D_{eff} is found to be inversely proportional to polymer molecular weight below and above the entanglement molecular weight.[4,5] This behavior contrasts with the inverse squared dependence on molecular weight of the equilibrium self-diffusion coefficient in an entangled melt. A molecular interpretation of these observations requires the theoretical treatment of the non-steady-state flow of polymers from a bulk melt into a confining medium. Although the flow of small molecules in porous media has been modelled under far-from-equilibrium conditions,[17–20] the flow of macromolecules into confining media under similar conditions has not received a comparable level of attention.

We have reported molecular dynamics simulations of the flow of a polymer melt into an initially evacuated rectangular slit.[21] In agreement with laboratory studies of intercalation kinetics in polymer-layered-silicates,[4,5] the simulation data were consistent with a diffusive description of the flow characterized by an effective diffusion coefficient D_{eff}, which decreased with increasing attraction of the slit walls for the polymer. In contrast with the laboratory results, however, D_{eff} in the simulations did not display an inverse molecular weight dependence. Increasing the chain length from $N=12$ to $N=120$ for a model[22] with an entanglement length $N_e \approx 35$ decreased D_{eff} by less than a factor of two. In a more recent work, we have extended this model to include the variation in slit width during intercalation and the presence of hydrocarbon chains grafted to the silicate surfaces.[23]

Since the flow of polymer into a narrow slit is necessarily influenced by the nature of the polymer-surface interaction, it is reasonable to assume that the effects of varying polymer molecular weight and polymer-surface interactions are coupled. In the present work, we report a systematic investigation of the effects of polymer molecular weight and polymer-surface interactions on the kinetics of polymer flow into a rectangular slit of fixed volume. As in Ref. 21, the polymer molecules are represented with the coarse-grained bead-spring model of Kremer and Grest.[22] The kinetic results are interpreted in terms of the nonequilibrium structure of polymer in the slit during the flow.

II. MODEL AND SIMULATION

Our simulation cell, which is composed of two compartments, is shown in Fig. 1. The left-hand compartment contains a reservoir of polymer melt, and is bounded on the left by a structureless wall parallel to the yz plane, which is maintained at constant pressure. The right-hand compartment contains two rigid blocks that form a slit of fixed volume that is empty at the start of each simulation. The direction of polymer flow from reservoir to slit is denoted the x direction. Periodic boundary conditions are applied in the y and z directions. The y and z dimensions of the reservoir vary with polymer length, but are chosen to ensure that no chain interacts with its own periodic image. The initial x dimension of the reservoir is chosen so that at the end of a simulation, the final x dimension is at least three radii of gyration. The x dimension of the slit is sufficiently large that polymers never reach the right-hand side on the simulation time scale. The geometry of the simulation cell employed here differs from that used in our earlier simulations.[21] There, a slit of finite

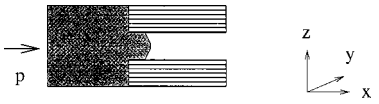

FIG. 1. The simulation cell is shown during polymer flow. The left-hand compartment contains a polymer melt maintained under constant external pressure, and the right-hand compartment contains an initially empty slit of infinite length.

length was connected to two reservoirs of polymer melt, one on each end, permitting the slit to fill and attain equilibrium with the reservoirs. The present geometry of a single reservoir allows us to examine the characteristics of individual trajectories, without the averaging inherent in the two-reservoir geometry.

The polymer chains are represented within the model of Kremer and Grest as soft-sphere beads connected by anharmonic FENE bonding potentials.[22] Nonbonded polymer beads interact through Lennard-Jones potentials that have been truncated at the minimum to produce a purely repulsive interaction. The Lennard-Jones energy scale and diameter for these interactions are denoted ϵ and σ, respectively. All dimensional quantities in this work will be expressed in Lennard-Jones units, in terms of ϵ, σ, and bead mass m. Polymer beads interact with the structureless confining wall of the reservoir through a Lennard-Jones potential averaged over the y and z directions, as in Ref. 21. The slit is formed from a rigid fcc lattice of spherical beads with the (1,1,1) surface parallel to the xy plane. Removal of two layers of particles from this lattice results in a slit whose z spacing, defined as the distance between the planes of centers of the particles forming the slit walls, is 2.9. A more meaningful measure of the width of the slit that is accessible to polymer beads is obtained by subtracting one lattice spacing in the z direction to yield an effective width of 1.9. Polymer beads interact with lattice particles with a Lennard-Jones potential characterized by length scale σ and energy ϵ_{bl}. In contrast to the bead–bead potential, the bead-lattice potential is cut off at a distance of 2.2 to include an attractive interaction. The bead-lattice interaction energy ϵ_{bl} is varied from 1 to 10. The external pressure on the wall bounding the reservoir is 5.23. The initial bead density in the reservoir is 0.85, and this value is approximately maintained during the flow into the slit. The polymer chain length varies from $N=4$ to $N=128$, and the total number of polymer beads varies from 2160 to 6912. A Brownian thermostat[21,22] maintains the system at constant temperature, $T=1.0$. The melt in the reservoir is equilibrated as described in Ref. 21.

III. RESULTS AND DISCUSSION

The influence of polymer-surface interactions on polymer flow is illustrated in Fig. 2, which shows the time dependence of the number of polymer beads in the slit, $n_s(t)$, for five different values of the polymer-surface interaction energy: $\epsilon_{bl}=1,3,5,7$, and 10. The chain length is $N=4$, and the y and z dimensions of the simulation cell are 6.2 and 5.8, respectively. The initial x dimension of the reservoir is 142.4 for $\epsilon_{bl}=1$ and is 71.2 in all other cases. Each curve shows the result of a single molecular dynamics trajectory. Two

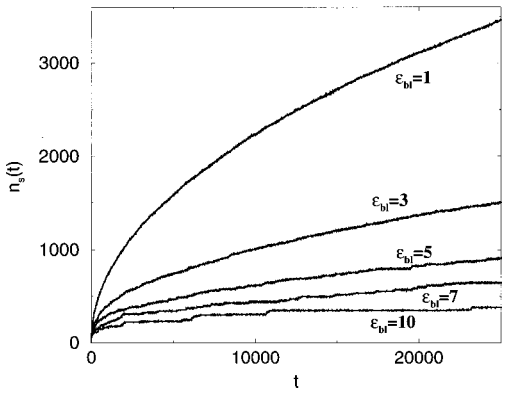

FIG. 2. The number of polymer beads in the slit, $n_s(t)$, is plotted versus time for chains of length $N=4$ for varying strengths of the polymer bead-surface interaction: $\epsilon_{bl}=1,3,5,7,10$.

trends are evident in Fig. 2. First, as the polymer-surface attraction increases, the flow rate decreases. This effect has been found in laboratory studies of nanocomposite formation,[5] and was observed in our previous simulations,[21] which treated the cases $\epsilon_{bl}=1$, 2, and 3. Increasing ϵ_{bl} increases the thermodynamic driving force for flow, but also increases the friction between surface and polymers.[15,16] It is evident that the kinetic effect dominates the thermodynamic one for this model. The second trend is the onset of a step and plateau structure in $n_s(t)$, as the polymer-surface interaction becomes more attractive. For $\epsilon_{bl}=1$, $n_s(t)$ is smooth within the resolution of the simulation, while for $\epsilon_{bl}=10$, the time dependence of $n_s(t)$ is characterized by steps and plateaus. Inspection of Fig. 2 shows that the onset of steps and plateaus with increasing ϵ_{bl} is gradual.

The coupled effects of varying chain length N and bead-surface interaction ϵ_{bl} are examined in Fig. 3, which shows $n_s(t)$ for $N=4$, 64(middle curve), and 128 with $\epsilon_{bl}=1$ [Fig. 3(A)], and for $N=4,16,64,128$ with $\epsilon_{bl}=5$ [Fig. 3(B)]. For $N=4$ and 16, the simulation cell has the dimensions employed above in Fig. 2, while for $N=64$ and 128, the y and z dimensions are 12.3 and 23.3 and the initial x dimension of

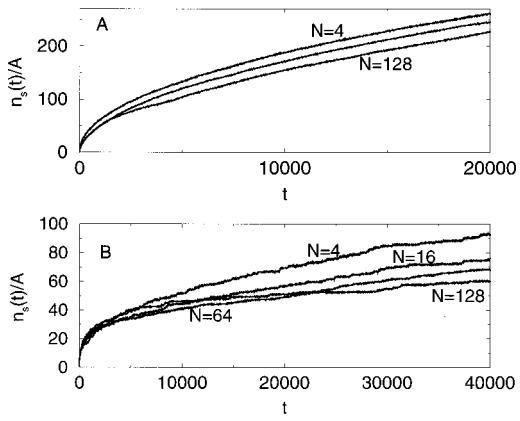

FIG. 3. The number of polymer beads in the slit, $n_s(t)$, normalized by the cross-sectional area of the slit, A, is plotted versus time for varying chain lengths and for two values of the polymer-surface interaction. In panel A, $N=4$, 64 (middle curve), and 128 with $\epsilon_{bl}=1$. In panel B, $N=4$, 16, 64, and 128 with $\epsilon_{bl}=5$.

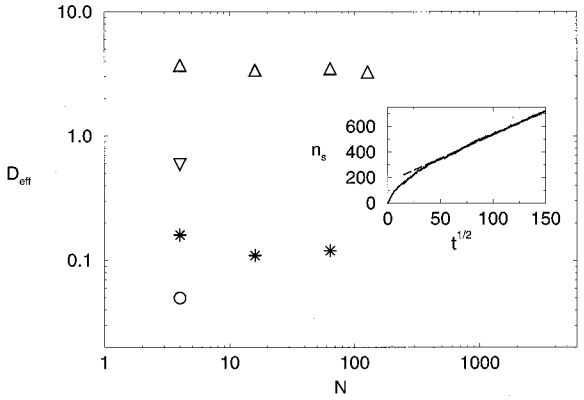

FIG. 4. Inset shows $n_s(t)$ for $\epsilon_{bl}=5$ and $N=16$, averaged over six trajectories to obtain a smooth curve, plotted versus $t^{1/2}$. The dashed line shows a fit to $n_s \propto t^{1/2}$. After an initial transient, $n_s \propto t^{1/2}$, permitting the extraction of a diffusion coefficient, D_{eff}. In the main section of this Figure, D_{eff} is shown for varying N and $\epsilon_{bl}=1$ (upward triangles), $\epsilon_{bl}=3$ (downward triangle), $\epsilon_{bl}=5$ (asterisks), and $\epsilon_{bl}=7$ (circle).

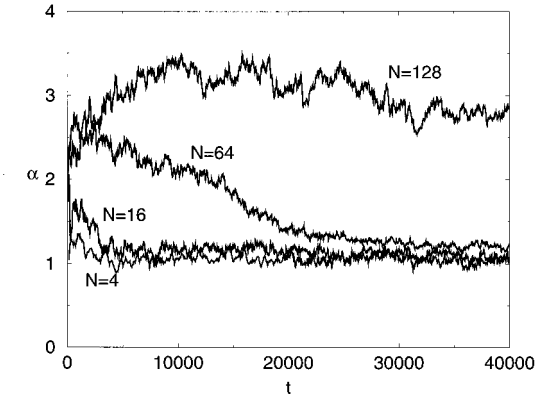

FIG. 5. The time evolution of the stretching of chains in the slit is quantified by the asymmetry parameter α, defined in Eq. (2), for chain lengths $N=4$, 16, 64, 128.

the reservoir is 28.3. To normalize the data, we plot $n_s(t)/A$, with A the cross-sectional area of the slit. We have checked that for the case $N=16$ and $\epsilon_{bl}=1$, $n_s(t)/A$ is independent of A for the two values employed in Fig. 3. Comparison of Figs. 3(A) and 3(B) shows that the N dependence of $n_s(t)$ varies with ϵ_{bl}. For the weaker polymer-surface attraction in Fig. 3(A), increasing N decreases the amount of material in the slit at a given time. However, even for chains of length 128, the time dependence of $n_s(t)$ is smooth, and does not show the step and plateau structure of Fig. 3(B). For the stronger polymer-surface interaction in Fig. 3(B), increasing N dramatically increases the duration of the plateaus in $n_s(t)$.

In our previous study of this model for weaker polymer-surface attractions,[21] we showed that for $N=12$ and $\epsilon_{bl}=1$, the flow of polymer into the slit could be approximately described with a diffusion equation, characterized by an effective diffusion coefficient, D_{eff}. For material entering a semi-infinite rectangular slit, diffusive flow implies

$$n_s(t)=2A\rho\sqrt{D_{\text{eff}}t/\pi}. \tag{1}$$

Equation (1) results from solving the diffusion equation under the assumption that the diffusion coefficient is infinite outside the slit, and is D_{eff} inside the slit.[21] This assumption presumes that the driven diffusion of beads just outside the slit is much faster than equilibrium self-diffusion in a bulk melt. In Eq. (1), the bead density in the reservoir is denoted ρ. The data in Fig. 3(A) do not show $t^{1/2}$ behavior at short times, but may be fit to this form after an initial transient. Such fitting yields values of D_{eff}[24] decreasing from 3.70 ± 0.2 for $N=4$ to 3.25 ± 0.2 for $N=128$. For comparison, the self-diffusion coefficient in the equilibrium melt varies from approximately 0.016 for $N=4$ to 0.0002 for $N=128$ at $T=1$ and $\rho=0.85$.[22] For the stronger polymer-surface attraction of Fig. 3(B), the plateau and step structure precludes fitting single trajectories to the form of Eq.(1). However, averaging several trajectories yields a smooth curve, as seen in the inset in Fig. 4, which shows $n_s(t)$ for $N=16$ and $\epsilon_{bl}=5$, averaged over six trajectories, plotted versus $t^{1/2}$. The dashed line shows a fit to $n_s \propto t^{1/2}$. This plot illustrates that after a transient, nondiffusive regime, $n_s(t)$ may be fit to a diffusive prediction. The values of D_{eff} obtained from such fitting for a variety of values of N and ϵ_{bl} are shown in Fig. 4. Upward triangles, the downward triangle, asterisks, and the circle indicate results for $\epsilon_{bl}=1$, 3, 5, and 7, respectively. The size of the symbol in each case is approximately equal to the uncertainty in the result. D_{eff} is seen in Fig. 4 to depend strongly on ϵ_{bl} and very weakly on N. Combining this analysis with the results shown in Figs. 3(A) and 3(B) shows that $n_s(t)$ is characterized by an initial nondiffusive regime that slows down with increasing chain length and whose duration increases with increasing chain length, followed by a diffusive regime that is nearly independent of chain length.

To interpret the origin of the initial nondiffusive regime, we examine the time-dependence of the structure of the chains as they traverse the slit. A measure of the deviation of chain structure from equilibrium is the average orientation of bonds in the slit. We quantify this orientation by an asymmetry parameter α, defined by

$$\alpha=\langle (x_{i+1}-x_i)^2/(y_{i+1}-y_i)^2\rangle, \tag{2}$$

with x and y indicating Cartesian components of bead displacements, and the indices labelling adjacent, bonded beads on a chain. The angular brackets indicate an average over all bonds in the slit. In a bulk melt at equilibrium, $\alpha=1$, while positive deviations from this value indicate chain stretching in the direction of flow. The time-dependence of the asymmetry parameter is plotted in Fig. 5 for the trajectories of Fig. 3(B). The shortest chains with $N=4$ and $N=16$ enter the slit with conformations that, on average, are stretched in the direction of flow. By the end of the simulation, this stretching has relaxed. For $N=64$, the stretching persists over a longer duration, and for the longest chains $N=128$, the chains remain significantly distorted away from equilibrium conformations over the entire course of the simulation. It is reasonable to assume that while the shapes of the molecules are changing significantly, a simple diffusion model will not hold. We therefore associate the transient nondiffusive behavior in $n_s(t)$ with the initial time period in Fig. 5 over which the chain shape is evolving. Figure 5 illustrates that the shapes of very long chains evolve differently from

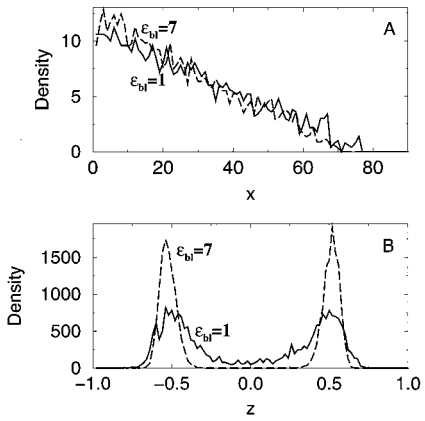

FIG. 6. Polymer bead density profiles in the flow direction (panel A) and across the slit (panel B) are shown for $\epsilon_{bl}=1$ (solid curves) and $\epsilon_{bl}=7$ (dashed curves). These profiles are defined to be linear densities, which are normalized so that integration over x in (A) and over z in (B) yields the number of beads in the slit. In each case 441 beads have entered the slit.

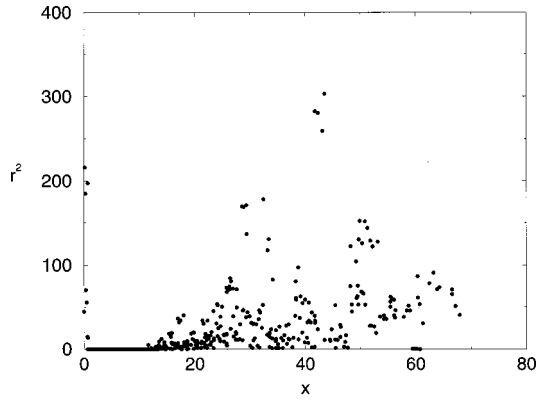

FIG. 7. Squared displacements of polymer beads over the time interval $9700<t<11\,300$ are shown as a function of initial distance of the bead from the slit entrance for $N=4$ and $\epsilon_{bl}=7$. This time interval corresponds to a plateau in Fig. 2. The slit entrance is sealed by a plug of immobile polymer beads.

those of shorter chains. For the case $N=128$, the chains continue to stretch during an initial transient, and then attain a stretched conformation which relaxes so slowly as to remain nearly constant during the course of the simulation. Thus for $N=128$, while the chain shape is roughly constant during the latter portion of the simulation, it remains far from the equilibrium structure.

The connection between nonequilibrium structure and dynamics is further explored in Fig. 6, which shows bead density profiles for $N=4$ with $\epsilon_{bl}=1$ (solid line) and 7 (dashed line). Panel A shows the bead density profiles in the flow direction, and panel B shows the bead density profiles across the slit. These density profiles are defined to be linear densities, which are normalized so that integration over x in Fig. 6(A) and over z in Fig. 6(B) yields the number of beads in the slit. The density profiles are measured at $t=362$ for $\epsilon_{bl}=1$ and at $t=10^4$ for $\epsilon_{bl}=7$. In each case, 441 beads have entered the slit. The density profiles along the flow direction in Fig. 6(A) are remarkably similar in the two cases. Fig. 6(B) shows that the beads are organized into two adsorbed layers, for both strong and weak polymer-surface interactions. While the layers become less diffuse with increasing ϵ_{bl}, the peak positions do not change significantly. The layering of confined fluids under both equilibrium and nonequilibrium conditions is well-established.[25–27]

Although Fig. 6 shows that nonequilibrium structure in the slit does not change dramatically with increasing ϵ_{bl}, the dynamics in the slit do show major differences for strongly and weakly attracting surfaces. Figure 7 shows the motion of individual beads for a case of strong polymer-surface attraction, $N=4$ and $\epsilon_{bl}=7$ over the time interval $9700<t<11\,300$. The squared displacement of each bead in the slit over this time interval, r^2, is plotted versus the initial distance of the bead from the slit edge. This time interval was chosen, because it represents a plateau in Fig. 2, during which the number of beads in the slit remains approximately constant. Figure 7 shows that beads near the slit entrance remain frozen during this plateau, while beads further in the slit are mobile. The frozen beads evidently form a plug, sealing off the entrance to the slit. During the subsequent stepwise increase in the number of beads from 441 to 454 at $t\approx 11\,500$, beads near the entrance of the slit have displacements on the order of one bead diameter. This analysis indicates that the beads forming a plug do not move until a critical stress is reached, and then move approximately as a unit over a fixed distance. This behavior is to be contrasted with the case of $N=4$ and $\epsilon_{bl}=1$, which is analyzed in Fig. 8 for the time interval $362<t<1962$, at the start of which the number of beads in the slit is also 441. In Fig. 8, beads near the entrance of the slit are mobile, and no plug exists.

Dynamical instabilities are commonly displayed by strongly driven fluids.[28–32] For instance, molecularly thin films respond to shear like a solid when deformed rapidly.[26] This solidlike response is characterized by alternation between periods during which the film is immobile and only deforms elastically, and periods during which the film rapidly rearranges in order to respond to the deformation.[33,34] Such a deformation occurs when a critical stress is exceeded. Solidlike or glassy behavior is observed for lower deformation rates as the film thickness decreases.[25,35] Increasing the affinity of the fluid for the surfaces also tends to produce

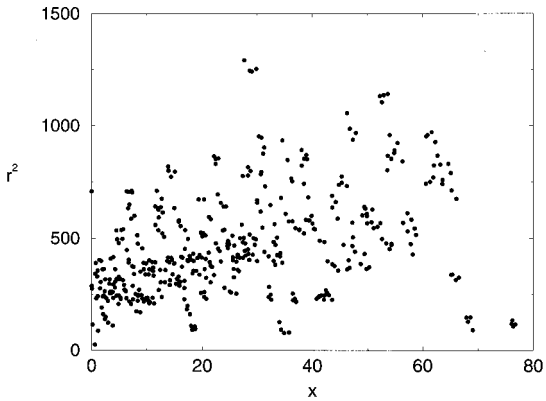

FIG. 8. The analysis of Fig. 7 is repeated for $N=4$ and $\epsilon_{bl}=1$ for the time interval $362<t<1962$. At $t=362$, the same number of beads occupy the slit as in Fig. 7. For this weaker polymer-surface interaction, no plug is formed.

glassy dynamics.[36] Our observations of the flow of a polymer melt into a narrow slit with attracting walls are consistent with the dynamics of other strongly driven fluid systems.

We have extended our earlier study of polymer flow into a narrow slit to investigate the effects of strong polymer-surface attractive interactions. We find that as the polymer-surface affinity is increased, the flow of material into the slit is slowed by kinetic effects, as has been observed in laboratory studies of the formation of layered nanocomposites by melt intercalation.[4,5] We observe a crossover in flow mechanism, from a flow that is approximately diffusive on the level of a single trajectory, to a stepwise filling mechanism characterized by the formation and relaxation of a plug at the slit entrance. We have also showed in the latter case by averaging only a small number of trajectories that a smooth time-dependence results, which may be fit to a diffusive model. The laboratory measurements on nanocomposite formation necessarily average over large numbers of slits, so we would not predict the observation of stepwise kinetics in those systems.[4,5] The N^{-1} dependence of D_{eff} observed in the laboratory is not a property of the model employed here, even for strong polymer-surface affinity. Interpreting this observation may require a model that includes the opening of the slit as it fills with polymer.[23] The analytical treatment of polymer flow under the strongly nonequilibrium conditions studied here remains an open issue. The observations reported here can form an empirical basis for such a treatment.

ACKNOWLEDGMENTS

We acknowledge support from the National Science Foundation, Division of Materials Research, through the Cornell Center for Materials Research. This research was conducted using the resources of the Cornell Theory Center, which receives funding from Cornell University, New York State, the National Center for Research Resources at the National Institutes of Health, and members of the Center's Corporate Partnership Program.

[1] E. P. Giannelis, Adv. Mater. **8**, 29 (1996).
[2] E. P. Giannelis, R. Krishnamoorti, and E. Manias, Adv. Polym. Sci. **138**, 107 (1999).
[3] E. P. Giannelis, Appl. Organomet. Chem. **12**, 675 (1998).
[4] R. A. Vaia, K. D. Jandt, E. J. Kramer, and E. P. Giannelis, Macromolecules **28**, 808 (1995).
[5] E. Manias, H. Chen, R. Krishnamoorti, J. Genzer, E. J. Kramer, and E. P. Giannelis (unpublished).
[6] R. A. Vaia and E. P. Giannelis, Macromolecules **30**, 7990, 8000 (1997).
[7] E. Hackett, E. Manias, and E. P. Giannelis, J. Chem. Phys. **108**, 7410 (1998).
[8] R. A. Vaia, R. K. Teukolsky, and E. P. Giannelis, Chem. Mater. **6**, 1017 (1994).
[9] D. K. Yang and D. B. Zax, J. Chem. Phys. **110**, 5325 (1999).
[10] D. K. Yang, R. A. Santos, H. Hegemann, E. P. Giannelis, E. Manias, and D. B. Zax (unpublished).
[11] Y. Kojima, A. Usuki, M. Kawasumi, A. Okada, Y. Fukushima, T. Kurauchi, and O. Kamigaito, J. Mater. Res. **8**, 1185 (1993).
[12] K. Yano, A. Usuki, M. Kawasumi, A. Okada, T. Kurauchi, and O. Kamigaito, J. Polym. Sci., Part A: Polym. Chem. **31**, 2493 (1993).
[13] Y. J. Liu, D. C. de Groot, J. L. Schindler, C. T. Kannewurf, and M. G. Kanatzidis, Chem. Mater. **3**, 992 (1991).
[14] P. B. Messersmith and S. I. Stupp, J. Mater. Res. **7**, 2599 (1992).
[15] Y. Lyatskaya and A. C. Balazs, Macromolecules **31**, 6676 (1998).
[16] A. C. Balazs, C. Singh, and E. Zhulina, Macromolecules **31**, 8370 (1998).
[17] R. F. Cracknell, D. Nicholson, and K. E. Gubbins, J. Chem. Soc., Faraday Trans. **91**, 1377 (1995).
[18] R. F. Cracknell, D. Nicholson, and N. Quirke, Phys. Rev. Lett. **74**, 2463 (1995).
[19] D. Nicholson, R. F. Cracknell, and N. Quirke, Langmuir **12**, 4050 (1996).
[20] E. J. Maginn, A. T. Bell, and D. N. Theodorou, J. Phys. Chem. **97**, 4173 (1993).
[21] J. Y. Lee, A. R. C. Baljon, R. F. Loring, and A. Z. Panagiotopoulos, J. Chem. Phys. **109**, 10321 (1998).
[22] K. Kremer and G. S. Grest, J. Chem. Phys. **92**, 5057 (1990).
[23] J. Y. Lee, A. R. C. Baljon, and R. F. Loring, J. Chem. Phys. (in press).
[24] The values of D_{eff} reported here for $\epsilon_{bl}=1$ are larger than the value of 3.0 reported in Ref. 21 for $N=12$ and $\epsilon_{bl}=1$. This apparent discrepancy arises from the different flow geometries employed in the two works. In Ref. 21, a slit of finite length was employed, while in the present work, a slit of effectively infinite length is used. In the latter case, extraction of a diffusion coefficient requires knowledge of the cross-sectional area of the slit, as can be seen from Eq. (1), while in the former case, this knowledge is not required.[21] Because the slit walls are formed of discrete, soft particles, the z dimension of the slit is not unambiguously defined. A larger estimate of the z dimension than that employed here would lower the values of D_{eff} reported here into the range quoted in Ref. 21.
[25] B. Bhushan, J. N. Israelachvili, and U. Landman, Nature (London) **374**, 607 (1995).
[26] A. L. Demirel and S. Granick, Phys. Rev. Lett. **77**, 2261 (1996).
[27] E. Manias, I. Bitsanis, G. Hadziioannou, and G. Ten Brinke, Europhys. Lett. **33**, 371 (1996).
[28] P. A. Thompson and M. O. Robbins, Phys. Rev. A **41**, 6830 (1990).
[29] M. J. Stevens, M. Mondollo, G. S. Grest, S. T. Cui, H. D. Crochan, and P. T. Cummings, J. Chem. Phys. **106**, 7303 (1997).
[30] U. Landman, W. D. Luedtke, and J. Gao, Langmuir **12**, 2514 (1996).
[31] S. Granick, Phys. Today **7**, 26 (1999).
[32] A. R. C. Baljon and M. O. Robbins, Comput. Theor. Polym. Sci. **9**, 35 (1999).
[33] P. A. Thompson and M. O. Robbins, Science **250**, 792 (1990).
[34] A. R. C. Baljon and M. O. Robbins, in *Micro/Nanotribology and its Applications*, *NATO Conference Proceedings*, edited by B. Bhushan (Kluwer Academic, Boston, 1996).
[35] P. A. Thompson, M. O. Robbins, and G. S. Grest, Isr. J. Chem. **35**, 93 (1995).
[36] R. K. Ballamudi and I. A. Bitsanis, J. Chem. Phys. **105**, 7774 (1996).